

# SCIENTIFIC REPORTS



OPEN

## Ultrasensitive colorimetric detection of circulating tumor DNA using hybridization chain reaction and the pivot of triplex DNA

Received: 06 December 2016

Accepted: 03 February 2017

Published: 09 March 2017

Ruimin Li\*, Li Zou\*, Yanwei Luo, Manjun Zhang & Liansheng Ling

This work presents an amplified colorimetric biosensor for circulating tumor DNA (ctDNA), which associates the hybridization chain reaction (HCR) amplification with G-Quadruplex DNAzymes activity through triplex DNA formation. In the presence of ctDNA, HCR occurs. The resulting HCR products are specially recognized by one sequence to include one GGG repeat and the other containing three GGG repeats, through the synergetic effect of triplex DNA and asymmetrically split G-Quadruplex forming. Such design takes advantage of the amplification property of HCR and the high peroxidase-like catalytic activity of asymmetrically split G-Quadruplex DNAzymes by means of triplex DNA formation, which produces color signals in the presence of ctDNA. Nevertheless, in the absence of ctDNA, no HCR happens. Thus, no triplex DNA and G-Quadruplex structure is formed, producing a negligible background. The colorimetric sensing platform is successfully applied in complex biological environments such as human blood plasma for ctDNA detection, with a detection limit corresponding to 0.1 pM. This study unambiguously uses triplex DNA forming as the pivot to integrate nucleic acid amplification and DNAzymes for producing a highly sensitive signal with low background.

Circulating tumor DNA (ctDNA), composed of small fragments of nucleic acid, has been demonstrated to be a promising biomarker for classification, diagnosis, and prognosis of cancers, which attracts much attention to develop techniques for monitoring ctDNA in blood<sup>1–3</sup>. Polymerase chain reaction (PCR) detection methodology represents a classical technology for quantifying ctDNA<sup>4</sup>, but it is costly and requires thermal cycling, complex, tedious steps and sophisticated instruments. Many isothermal nucleic acid amplification techniques, including rolling-circle amplification (RCA)<sup>5</sup>, strand-displacement amplification (SDA)<sup>6</sup>, helicase-dependent amplification (HAD)<sup>7</sup> and hybridization chain reaction (HCR)<sup>8</sup> have the potential to revolutionize detection and monitoring of ctDNA. Among them, HCR, an enzyme-free amplification technique, has superior strengths, such as, less hassle in operating conditions, cost effectiveness, sensitivity and simplicity<sup>9,10</sup>. Based on HCR amplification, a variety of targets have been successfully determined, including nucleic acids, small molecules and proteins<sup>11–13</sup>.

For instance, Miao *et al.* proposed two strategies for miRNA detection based on hybridization chain reaction. One took advantage of the strategy that analyte triggered nanoparticle localization on a tetrahedral DNA modified followed by HCR amplification<sup>14</sup>, the other is based on HCR-mediated localized surface plasmon resonance (LSPR) variation of silver nanoparticles (AgNPs)<sup>15</sup>. Xie *et al.* developed an aptasensor assay for lipopolysaccharides based on HCR<sup>16</sup>. Zou *et al.* reported a universal platform for nucleic acids, small molecules and proteins, which integrated HCR with the assembly of gold nanoparticles (AuNPs)<sup>17</sup>. Although there are many advances about HCR in the design of biomarker assays, it still needs to develop new methods, which can efficiently amplify target and produce a highly sensitive signal with zero background.

Here, we proposed an amplified colorimetric strategy for highly selective and sensitive detection of the ctDNA, which employed the triplex forming oligonucleotides (TFOs) to specially recognize the dsDNA products of HCR and synergistically form the asymmetrically split G-Quadruplex structure. The resulting G-Quadruplex structure bound with hemin and formed the asymmetrically split G-quadruplex/hemin complex with high peroxidase-like activity, which catalyzed the oxidation-reduction reaction of 2,2'-azino-bis(3-ethylbenzothiazoline-6-sulfonic acid) (ABTS<sup>2-</sup>) and H<sub>2</sub>O<sub>2</sub>, and yielded the green radical anion (ABTS<sup>-</sup>) and H<sub>2</sub>O. Consequently, a detectable

School of Chemistry, Sun Yat-Sen University, Guangzhou 510275, P. R. China. \*These authors contributed equally to this work. Correspondence and requests for materials should be addressed to L.L. (email: cesllsh@mail.sysu.edu.cn)

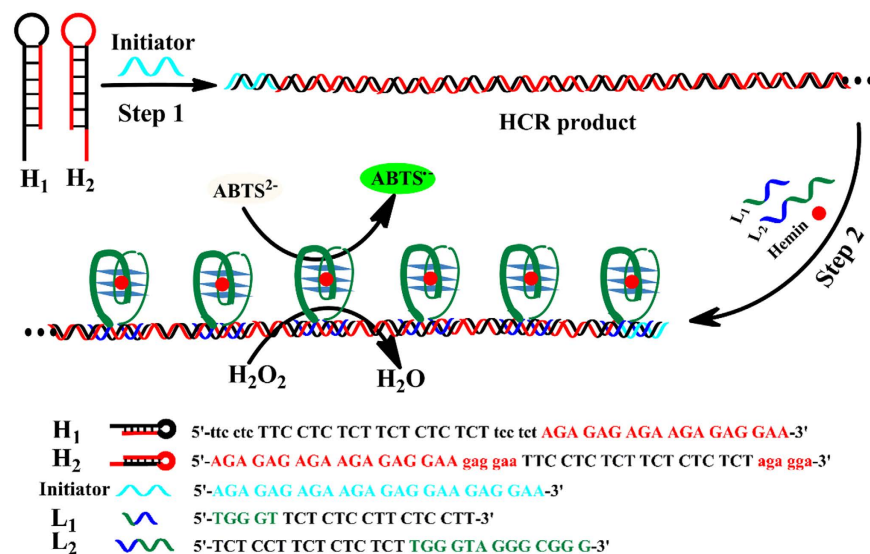


**Figure 1. Schematic illustration of amplified colorimetric nucleic acid detection.**

color change was achieved by the naked eye or with a spectrophotometer. To the best of our knowledge, we have for the first time used the triple-helix DNA forming technique to combine the HCR products and the asymmetrically split guanine-rich DNA sequences, and achieved colorimetric and visual detection of the ctDNA sequence with highly sensitive signal and negligible background.

## Results and discussion

**Principle of the proposed method.** The principle of the proposed colorimetric sensing system is depicted in Fig. 1. It involves five oligonucleotides, H<sub>1</sub>, H<sub>2</sub>, Initiator, L<sub>1</sub> and L<sub>2</sub>. H<sub>1</sub> and H<sub>2</sub> are designed to contain the hairpin structures and have 18-base stems, 6-base loops and 6-base sticky ends, which are stable and have no chance to hybridize with each other at room temperature. When the sequence Initiator is introduced in the system, the steady state of H<sub>1</sub> and H<sub>2</sub> is disturbed by the hybridization of Initiator and H<sub>1</sub>, and then triggering a chain reaction for alternating addition of these two hairpins, yielding a chain-like assembly of H<sub>1</sub> and H<sub>2</sub>. The HCR product with a strict duplex formation has an iterative 30-base homopyrimidine-homopurine duplex DNA region, which is specifically recognized by a third homopyrimidine or homopurine single-strand DNA by Hoogsteen or reverse Hoogsteen hydrogen resulting in the structure of triplex DNA. The sequence L<sub>1</sub> has two portions, a portion with 15-base homopyrimidine, which has the capability of sequence-specific recognition of the major groove of homopyrimidine-homopurine duplex DNA of HCR product, the other portion with the one-fourths of the G-quadruplex sequence. Similarly, L<sub>2</sub> also has two functional parts, one part with 15-base homopyrimidine that can recognize homopyrimidine-homopurine duplex DNA of HCR product and form the triplex DNA, the other one to include the three-fourths of the G-quadruplex sequence<sup>18</sup>. Under certain conditions, the homopyrimidine parts in L<sub>1</sub> and L<sub>2</sub> specially recognize the major groove of homopyrimidine-homopurine dsDNA in the HCR product. Based on the simple rule of complementary Hoogsteen hydrogen bonding, the triplets, CG-C<sup>+</sup> and TA-T, are obtained<sup>19</sup>. In other words, the triplex DNA is successfully formed by HCR products, L<sub>1</sub> and L<sub>2</sub>. Meanwhile, the two asymmetrically split parts in L<sub>1</sub> and L<sub>2</sub> assemble to form a special G-quadruplex structure. The special G-quadruplex structure can bind with hemin and form the asymmetrically split G-quadruplex/hemin complex with high peroxidase-like activity, which can catalyze the reaction of ABTS<sup>2-</sup> and H<sub>2</sub>O<sub>2</sub>. Thus, a detectable color change is achieved by the naked eye or with a spectrophotometer.

**Feasibility of the proposed method.** To clearly demonstrate the triplex DNA forming by L<sub>1</sub>, L<sub>2</sub> and HCR products, we chose the iterative 30-base homopyrimidine-homopurine duplex DNA region in HCR products as the target dsDNA, as shown in Fig. 2a. In the presence of dsDNA, L<sub>1</sub> and L<sub>2</sub> recognized the major groove of homopyrimidine-homopurine. Through the synergistic effect, the triplex DNA and asymmetrically split G-quadruplex configurations were formed by dsDNA, L<sub>1</sub> and L<sub>2</sub>. The special G-quadruplex structure bound with hemin and became an active DNzyme. As depicted in Fig. 2b, in the absence of dsDNA, the absorbance value of the oxygenation product ABTS<sup>•-</sup> at 420 nm was about 0.1 at the 180 seconds time point. However, in the presence of dsDNA, the value was about 1.2. Therefore, it indicated that the two asymmetrically split G-rich parts of L<sub>1</sub> and L<sub>2</sub> assembled to form an active G-quadruplex structure in the presence of the homopyrimidine-homopurine sequences dsDNA. Furthermore, to investigate the configuration change of this process, we carried out the native polyacrylamide gel electrophoresis (PAGE) under different conditions, with dsDNA, L<sub>1</sub> and L<sub>2</sub> as the controls. As exhibited in Fig. 2c, in the absence of dsDNA, L<sub>1</sub> and L<sub>2</sub> had no connection with each other (lane 5). By the introduction of dsDNA, the resulting triplex DNA products, dsDNA: L<sub>1</sub> (lane 6), dsDNA: L<sub>2</sub> (lane 7), dsDNA: L<sub>1</sub> : L<sub>2</sub> (lane 8), were obtained. Since the homopyrimidine parts in L<sub>1</sub> and L<sub>2</sub> had the ability of sequence-specific recognition of the major groove of homopyrimidine-homopurine dsDNA. Thus, the rationale that introduced the

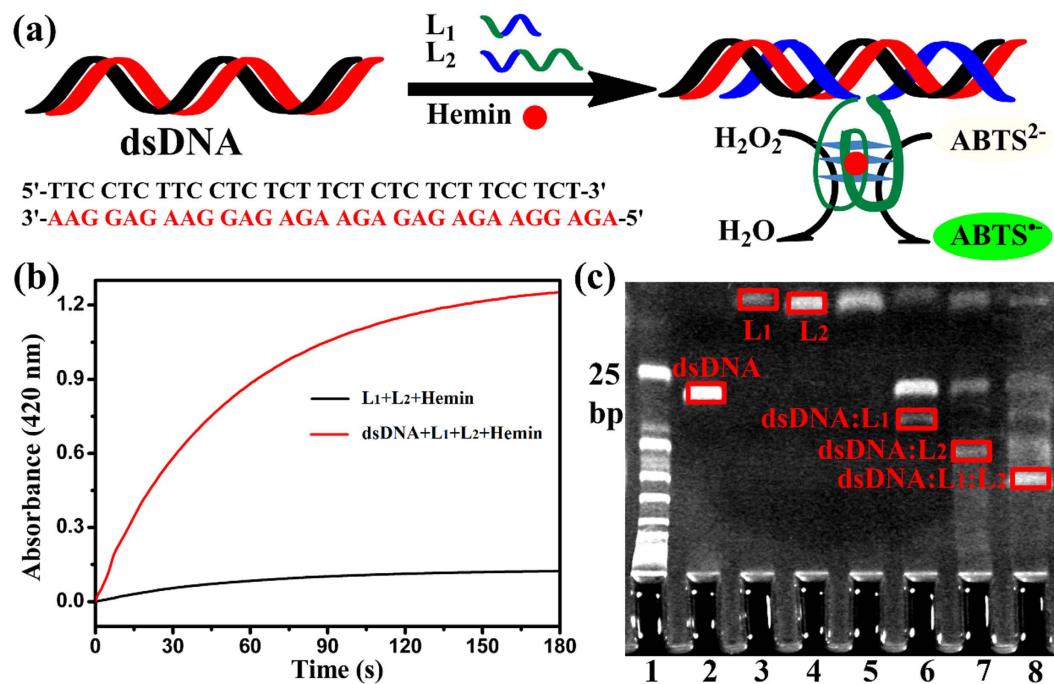


**Figure 2.** (a) Analysis of the iterative (dsDNA) in HCR products by L<sub>1</sub> and L<sub>2</sub> that produced the triplex DNA and asymmetrically split G-quadruplex configurations through the synergistic effect. (b) Comparison of time-dependent absorbance changes of ABTS<sup>2-</sup> upon the absence (black) and presence (red) of dsDNA. (c) The effect of the triplex DNA forming by L<sub>1</sub>, L<sub>2</sub> and the iterative (dsDNA) in HCR products. Lane 1, 25-bp ladder marker; lane 2, 0.5 μM dsDNA; lane 3, 1 μM L<sub>1</sub>; lane 4, 1 μM L<sub>2</sub>; lane 5, 1 μM L<sub>1</sub> and 1 μM L<sub>2</sub>; lane 6, 0.5 μM dsDNA and 1 μM L<sub>1</sub>; lane 7, 0.5 μM dsDNA and 1 μM L<sub>2</sub>; lane 8, 0.5 μM dsDNA, 1 μM L<sub>1</sub> and 1 μM L<sub>2</sub>.

asymmetrically split G-quadruplex/hemin DNAzymes as the catalyst of producing signals with the aid of forming triplex DNA had certain feasibility.

To ensure the success of HCR reaction as designed, the agarose gel electrophoresis assay was employed. As depicted in Fig. 3a, from lane 1, lane 2, lane 3 to lane 4, the concentrations of Initiator DNA were 0.0 μM, 1.0 μM, 0.4 μM, 0.1 μM, respectively. In the absence of Initiator, the HCR reaction could not carry out because there was only one band of H<sub>1</sub> and H<sub>2</sub>. By the addition of different concentration Initiator, the HCR reactions took place, and the band of H<sub>1</sub> and H<sub>2</sub> disappeared. It was noted that the concentration of Initiator was lower, the length of HCR products was longer. It suggested that higher concentration of Initiator opened more H<sub>1</sub>, which led more parallel polymerization reactions to carry out at the same time, generating shorter HCR products, which was in good accordance with some previous literatures<sup>20–22</sup>. In order to verify the feasibility of the proposed method, the H<sub>2</sub>O<sub>2</sub>-ABTS<sup>2-</sup> reactions were investigated under different conditions. (Figure 3b) The absorbance of the mixture of H<sub>2</sub>O<sub>2</sub> and ABTS<sup>2-</sup> had little change within 180 s (curve (1)). Similarly, by the addition of hemin (Fe-protoporphyrin IX), an iron-containing prosthetic group among a diverse group of proteins, with weak peroxidase-like activity, the absorbance of the mixture H<sub>2</sub>O<sub>2</sub> and ABTS<sup>2-</sup> also had inappreciable change within 180 s as well (curve (2))<sup>23,24</sup>. In the absence of Initiator, the absorbance of the mixture H<sub>1</sub>, H<sub>2</sub>, L<sub>1</sub>, L<sub>2</sub>, hemin, H<sub>2</sub>O<sub>2</sub> and ABTS<sup>2-</sup> had weak change within 180 s (curve (3)), due to the mildly enhanced peroxidase-like activity of hemin by abridged guanine-rich single-strand sequences L<sub>2</sub> possessing three GGG repeats. Upon addition of Initiator, the absorbance of the mixture H<sub>1</sub>, H<sub>2</sub>, L<sub>1</sub>, L<sub>2</sub>, hemin, H<sub>2</sub>O<sub>2</sub> and ABTS<sup>2-</sup> occurred obvious change (curve (4)). These results suggested that Initiator disturbed the steady state of H<sub>1</sub> and H<sub>2</sub>. The resulting HCR products were successfully recognized by L<sub>1</sub> and L<sub>2</sub>. Through the synergistic effect, the triplex DNA and asymmetrically split G-quadruplex configurations were formed. The special G-quadruplex structure bound with hemin and formed the asymmetrically split G-quadruplex/hemin complex with high peroxidase-like activity, which could catalyze ABTS<sup>2-</sup> and H<sub>2</sub>O<sub>2</sub>. The colored signals visible to the naked eye were in good accordance with that of the absorbance changes at 420 nm. Therefore, the proposed strategy was feasibility and it worked as designed.

Circular dichroism (CD) spectroscopy has great superiority in exploring the DNA configuration. To further understand the principle of the proposed assay, CD spectroscopy was measured under different cases. As displayed in Fig. 3c, there was no apparent characteristic peak for H<sub>1</sub> + H<sub>2</sub>, L<sub>1</sub>, L<sub>2</sub>, L<sub>1</sub> + L<sub>2</sub>, respectively. However, by the addition of Initiator, the CD spectroscopy of H<sub>1</sub> + H<sub>2</sub> had a positive cotton effect peak at about 218 nm, an enhanced positive peak at about 270 nm and negative peak at about 242 nm. It indicated that Initiator triggered the HCR between H<sub>1</sub> and H<sub>2</sub>, and produced a chain-like assembly of H<sub>1</sub> and H<sub>2</sub>. Moreover, by the introduction of L<sub>1</sub> and L<sub>2</sub>, the CD spectroscopy of the mixture (Initiator + H<sub>1</sub> + H<sub>2</sub>) had an obvious negative peak appeared at about 210 nm, which was characterized as the forming of triplex DNA<sup>25,26</sup>. There was a positive peak near 270 nm and negative band around 240 nm in the CD spectroscopy of Initiator + H<sub>1</sub> + H<sub>2</sub> + L<sub>1</sub> + L<sub>2</sub>, suggesting that the typical parallel G-quadruplex structures were formed by L<sub>1</sub> and L<sub>2</sub> with the help of triplex forming<sup>27</sup>.

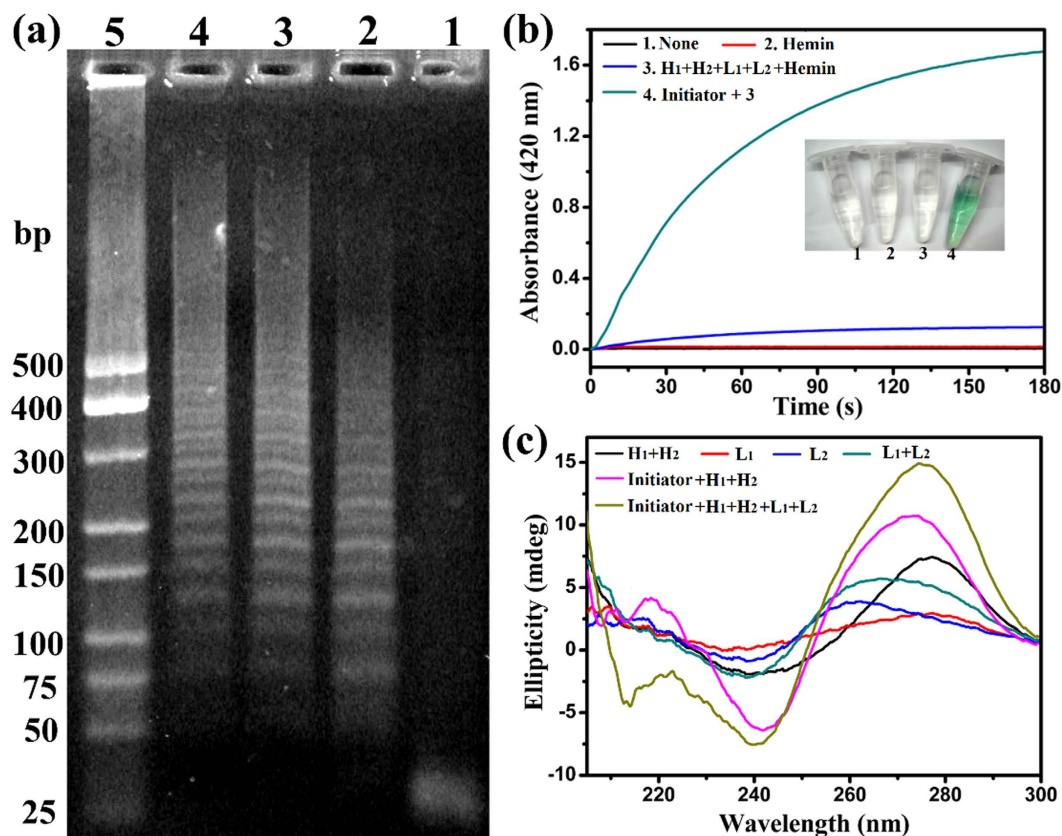


**Figure 3.** (a) Effect of Initiator concentrations on HCR. Lane 1-4, four different concentrations of Initiator (0.0  $\mu\text{M}$ , 1.0  $\mu\text{M}$ , 0.4  $\mu\text{M}$  and 0.1  $\mu\text{M}$ ) in the mixture of 1.0  $\mu\text{M}$   $\text{H}_1$  and 1.0  $\mu\text{M}$   $\text{H}_2$ ; lane 5, 25-bp ladder marker. (b) The time-dependent absorbance changes of the  $\text{H}_2\text{O}_2$ - $\text{ABTS}^{2-}$  reactions in different conditions and corresponding color changes. (10 nM Initiator, 0.2  $\mu\text{M}$   $\text{H}_1$ , 0.2  $\mu\text{M}$   $\text{H}_2$ , 0.4  $\mu\text{M}$   $\text{L}_1$ , 0.4  $\mu\text{M}$   $\text{L}_2$ , 0.4  $\mu\text{M}$  hemin, 2.0 mM  $\text{H}_2\text{O}_2$  and 0.2 mM  $\text{ABTS}^{2-}$ ) (c) Circular dichroism (CD) spectroscopy in different cases. (5  $\mu\text{M}$  Initiator, 5  $\mu\text{M}$   $\text{H}_1$ , 5  $\mu\text{M}$   $\text{H}_2$ , 10  $\mu\text{M}$   $\text{L}_1$ , 10  $\mu\text{M}$   $\text{L}_2$ ).

**Effect of the experimental conditions.** The proposed colorimetric sensing system was established based upon recognizing and detecting the HCR product by means of synergy effect of triplex DNA and the asymmetrically split G-quadruplex forming, which bound with hemin and catalyzed the reaction of  $\text{ABTS}^{2-}$  and  $\text{H}_2\text{O}_2$ . Herein, some key factors included in the system may affect the sensitivity of the colorimetric assay, such as the temperature and pH of the reaction solution, concentrations of  $\text{H}_2\text{O}_2$ ,  $\text{ABTS}^{2-}$ , spermine and  $\text{Ag}^+$ . Upon the optimization, temperature of the reaction solution, pH value of Tris-Ac buffer, the concentrations of  $\text{H}_2\text{O}_2$ ,  $\text{ABTS}^{2-}$ , spermine and  $\text{Ag}^+$  were 25  $^\circ\text{C}$ , pH 7.4, 2.0 mM, 0.20 mM, 0.25 mM, 0.15  $\mu\text{M}$ , respectively (Fig. 4). The details were depicted in Supplementary Information.

**Sensitivity of the proposed method.** Under optimal experimental conditions, the sensitivity and dynamic range of the colorimetric HCR assay were evaluated toward Initiator standards in 20 mM Tris-Ac, pH 7.4, 25  $^\circ\text{C}$  containing 2.0 mM  $\text{H}_2\text{O}_2$ , 0.20 mM  $\text{ABTS}^{2-}$ , 0.25 mM Spermine, 0.15  $\mu\text{M}$   $\text{Ag}^+$ , 0.10 M  $\text{K}^+$ , 0.40  $\mu\text{M}$  hemin, 0.20  $\mu\text{M}$   $\text{H}_1$ , 0.20  $\mu\text{M}$   $\text{H}_2$ , 0.40  $\mu\text{M}$   $\text{L}_1$  and 0.40  $\mu\text{M}$   $\text{L}_2$ . Figure 5a displayed the time-dependent absorbance changes of  $\text{ABTS}^{2-}$  upon different concentrations of Initiator. When the concentration of Initiator was higher, the absorbance changes increased in their intensities. In the absence of Initiator, feeble absorbance change was observed. Thus, the blank response of the time-dependent absorbance changes of  $\text{ABTS}^{2-}$  was negligible. The calibration curve corresponding to the absorbance changes observed after a fixed time interval of 180 s upon analysis of different concentrations of Initiator was described in Fig. 5b. The calibration plots (Fig. 5b, Inset) exhibited a linear relationship between the absorbance value of the oxygenation product  $\text{ABTS}^{2-}$  ( $\lambda_{\text{max}} = 420 \text{ nm}$ ) and the logarithm of Initiator concentrations in the range from 0.5 pM to 500 pM, the linear regression equation was  $A = 0.2094 \log(C_{\text{Initiator}}/\text{pM}) + 0.2743$ , where A was the absorbance value of  $\text{ABTS}^{2-}$  ( $\lambda_{\text{max}} = 420 \text{ nm}$ ) at the 180 seconds time point,  $C_{\text{Initiator}}$  was the concentration of Initiator. The correlation coefficient R was 0.9937. The detection limit was 0.1 pM ( $3\sigma/\text{slope}$ ). Compared to the previously reported DNA colorimetric sensing strategies (as shown in Supplementary Table S1)<sup>13,17,28,29</sup>, the present work possessed high sensitivity.

**Generality of the proposed method.** The proposed method is able to detect other nucleic acid sequences, including miRNA and DNA, with the aid of elaborately designed hairpin Capture probes (as shown in Fig. 6). The Capture probe consists of two main parts. One is the Target recognition element represented by pink color,

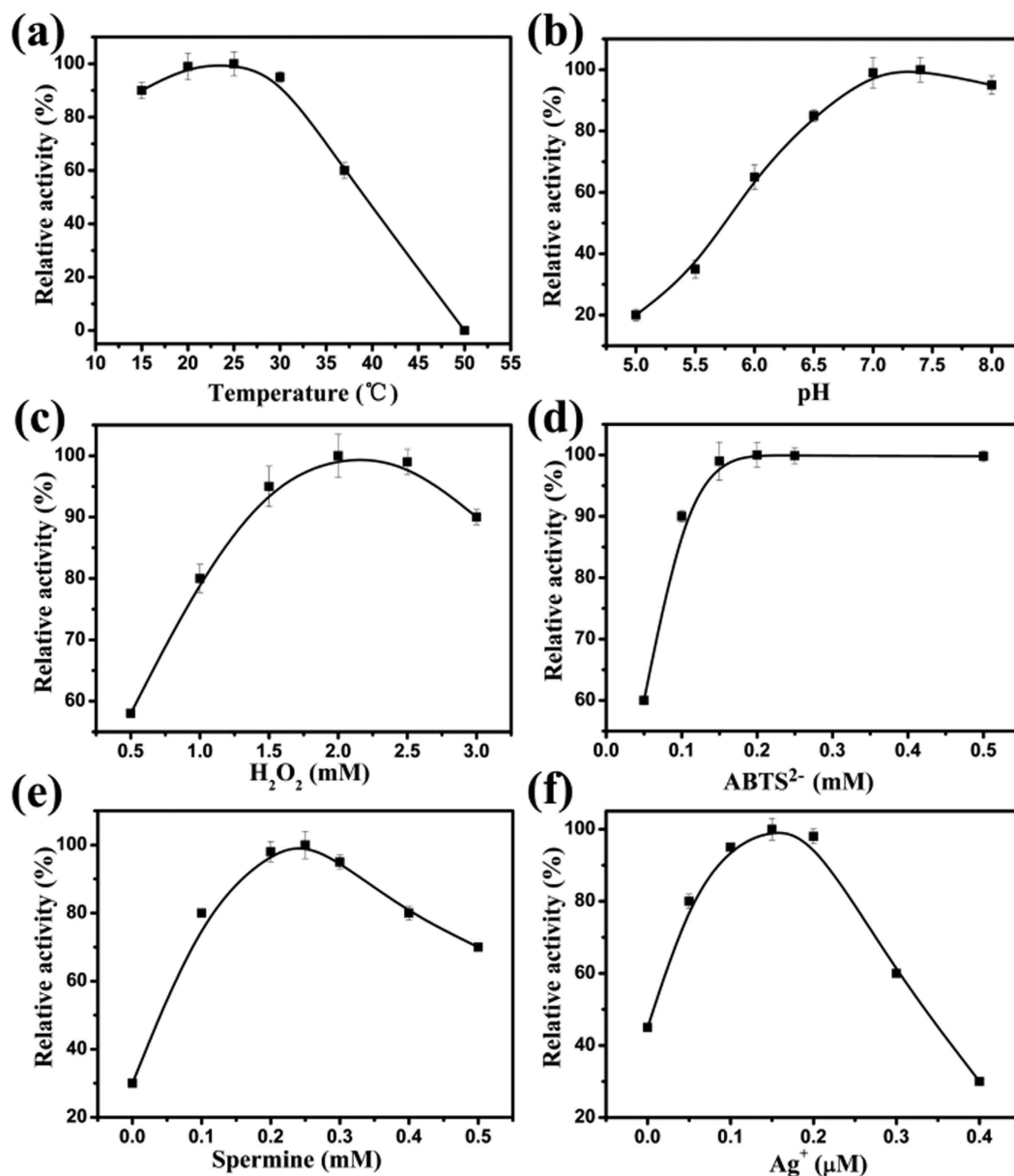


**Figure 4.** Effect of different conditions on the time-dependent absorbance changes of the  $\text{H}_2\text{O}_2$ -ABTS $^{2-}$  reactions, involving the temperature of the reaction solution (a), pH value of Tris-Ac buffer (b), concentrations of  $\text{H}_2\text{O}_2$  (c), ABTS $^{2-}$  (d), spermine (e) and  $\text{Ag}^+$  (f). The error bars represent the standard deviation of the three measurements. The optimal point in each curve was set as 100%.

which is in the stem and sticky end of the hairpin Capture probe, in order to easily recognized Target nucleic acid sequence. The other is the Signal amplification element expressed in red color, which mainly concentrates in the loop of the Capture hairpin structure, to avoid non-specifically triggering HCR. In the absence of Target nucleic acid sequence, the Signal amplification DNA sequence is firmly locked in the hairpin Capture probe. Thus, no HCR happens and no color change is discovered. In the presence of Target nucleic acid sequence, the Capture hairpin structure is opened and the Signal amplification DNA sequence is released. Hence, HCR takes place and the characteristic green color is observed. These suggest the generality of the proposed method in nucleic acid detection. Furthermore, the proposed method can be extended to assay other targets, by using aptamer technology, such as small molecules, proteins and cells<sup>30–32</sup>.

**Circulating tumor DNA (ctDNA) detection.** As a proof-of-concept, a circulating tumor DNA (ctDNA) was chosen as the model analyte of interest, which was a remarkable biomarker due to the high frequency of mutations of the PIK3CA gene in breast cancer (PIK3CA E542 KM (c.1624 G > A), 5'-AGT GAT TTT AGA GAG AG-3')<sup>33</sup>. The hairpin DNA sequence (5'-AGA GAG AGA AGA GAG GAA CTC TT CT CTC TCT AAA ATC ACT-3') was introduced as Capture probe to recognize ctDNA. In the presence of ctDNA, the Capture

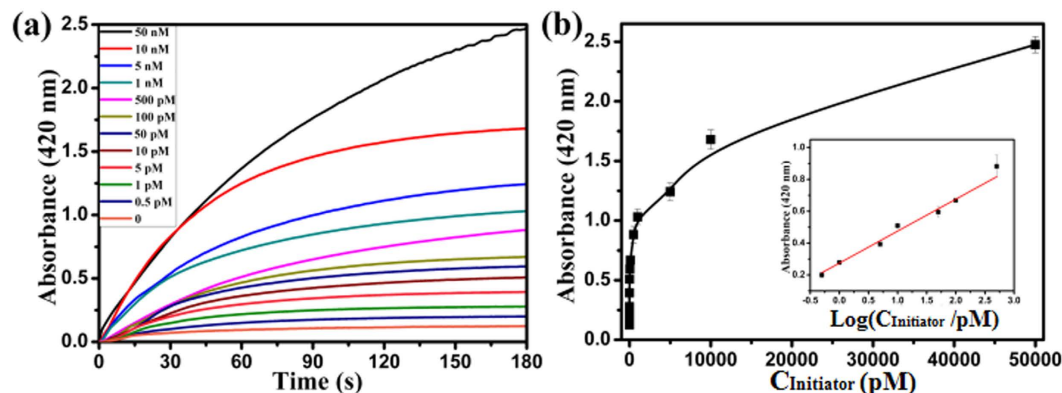


**Figure 5.** (a) The time-dependent absorbance changes of  $\text{ABTS}^-$  corresponding to different concentrations of Initiator. (b) The calibration curve of the absorbance changes observed after a fixed time interval of 180 s vs variable concentrations of Initiator. Inset shows the linear relationship between the absorbance value of the oxygenation product  $\text{ABTS}^-$  ( $\lambda_{\text{max}} = 420 \text{ nm}$ ) at the 180 seconds time point and the logarithm of Initiator concentrations. The error bars represent the standard deviation of the three measurements.

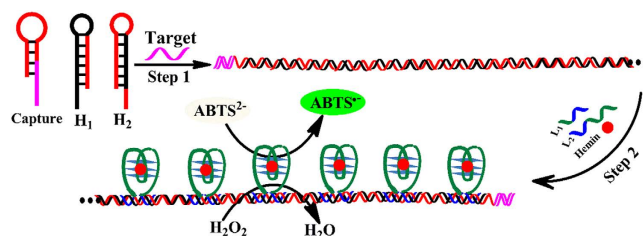


**Figure 6.** The generality of the proposed method for other nucleic acid sequences.

probe was opened and released a single-strand DNA sequence, which initiated the cross-opening of hairpins  $\text{H}_1$  and  $\text{H}_2$ . The chain-like HCR products were characterized by the agarose gel electrophoresis assay. As depicted in Supplementary Figure S1, lane 1 only contained  $1.0 \mu\text{M}$  Capture, lane 2 had  $1.0 \mu\text{M}$  Capture and  $1.0 \mu\text{M}$  ctDNA. In the presence of  $1.0 \mu\text{M}$  Capture,  $1.0 \mu\text{M}$   $\text{H}_1$ , and  $1.0 \mu\text{M}$   $\text{H}_2$ , the concentrations of ctDNA from lane 3, lane 4, lane 5 to lane 6, were  $0.0 \mu\text{M}$ ,  $1.0 \mu\text{M}$ ,  $0.4 \mu\text{M}$ ,  $0.1 \mu\text{M}$ , respectively. It suggested that by the addition of ctDNA, the Capture was opened and released a single-strand DNA sequence which initiated the HCR reaction. Figure 7a depicted the time-dependent absorbance changes of  $\text{ABTS}^-$  upon analysis of different concentrations of ctDNA. As the concentration of ctDNA was lower, the absorbance changes weakened in their intensities. In the absence of ctDNA, the blank response of the time-dependent absorbance changes of  $\text{ABTS}^-$  could be negligible. The calibration curve corresponding to the absorbance changes observed after a fixed time interval of 180 s upon analysis of different concentrations of ctDNA was described in Fig. 7b. The absorbance value of  $\text{ABTS}^-$  ( $\lambda_{\text{max}} = 420 \text{ nm}$ ) at the 180 seconds time point showed a good linear correlation with the logarithm of ctDNA concentrations in the range from  $0.5 \text{ pM}$  to  $500 \text{ pM}$ , with a detection limit as low as  $0.1 \text{ pM}$  ( $3\sigma/\text{slope}$ ) and the correlation coefficient  $R$  0.9956. Compared to some other reported ctDNA detection methods (as shown in Supplementary Table S2)<sup>33–35</sup>, this approach has the following good performances: (1) With the aid of triple-helix DNA forming, the HCR amplification and the high peroxidase-like catalytic activity of the G-Quadruplex DNAzymes are combined, and thus, high sensitive colorimetric signals can be achieved for ctDNA detection. (2) The signatures of enzyme-free and visualization give this approach a potential for point-of-care testing in clinical analysis.

To validate the specificity of ctDNA detection system, three sequences of the one-, two-, and three-base mutations ctDNA (1), ctDNA (2), and ctDNA (3), respectively, were prepared as analytes to test. Figure 7c depicted the time-dependent absorbance changes of  $\text{ABTS}^-$  upon analysis of ctDNA, ctDNA (1), ctDNA (2), ctDNA (3), all at a concentration of  $500 \text{ pM}$ , and without any analytes. The calibration column corresponding to the absorbance changes observed after a fixed time interval of 180 s was demonstrated in Fig. 7d. The spectral changes of the two-base and three-base mismatched analytes ctDNA (2) and ctDNA (3) were almost identical to the background signal of the system. However, the one-base mismatched ctDNA (1) was easily distinguished from ctDNA. It suggested that the system had high selectivity.

To evaluate the feasibility of the assay in real samples, human blood plasma samples voluntarily provided by healthy people were tested and the DNA extraction procedures from blood plasma were described in *Methods*. To detect ctDNA in human blood plasma samples, 1: 10 dilution of human blood plasma samples was analyzed alone or spiked with  $10 \text{ pM}$ ,  $50 \text{ pM}$  and  $100 \text{ pM}$  ctDNA. As shown in Table 1, the obtained results corresponded with the same concentrations provided in Tris-Ac buffer. The relative standard deviations (RSDs) for the three samples were all below 6%, exhibiting the adequate accuracy and good reproducibility of the present sensing strategy. It

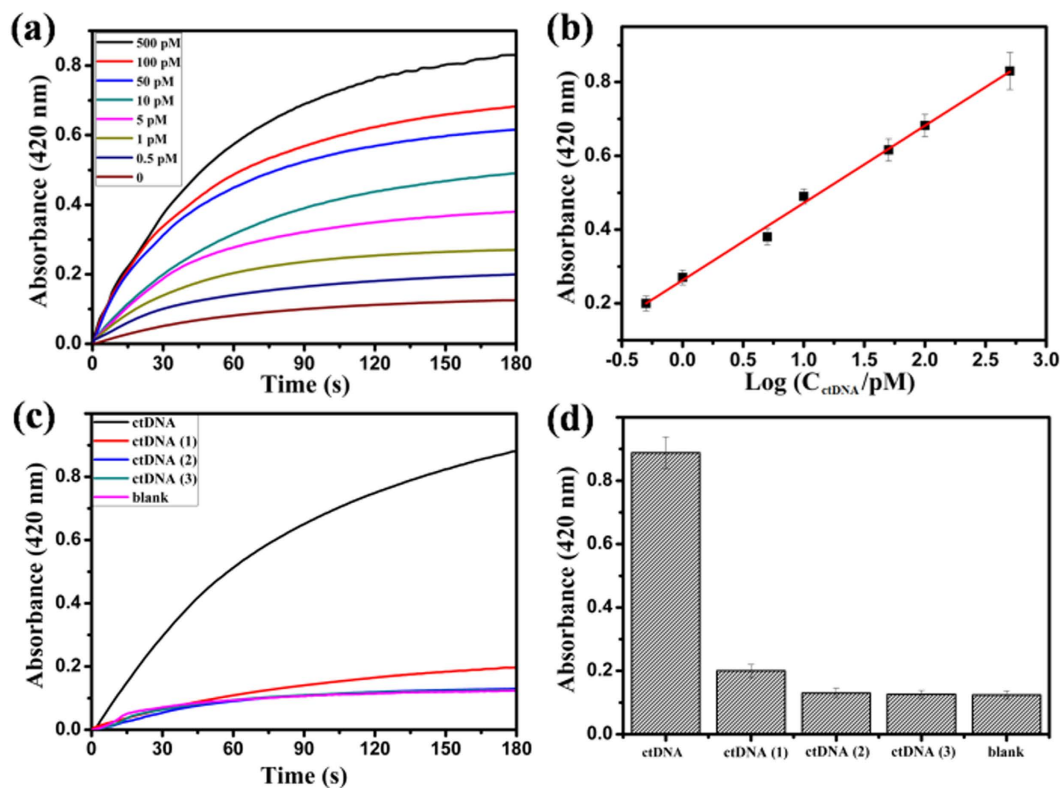


**Figure 7.** (a) The time-dependent absorbance changes of  $\text{ABTS}^-$  corresponding to different concentrations of ctDNA. (b) The linear relationship between the absorbance value of the oxygenation product  $\text{ABTS}^-$  ( $\lambda_{\text{max}} = 420 \text{ nm}$ ) at the 180 seconds time point and the logarithm of ctDNA concentrations. (c) Time-dependent absorbance changes upon analysis of different analytes: ctDNA, 500 pM; ctDNA (1), one-base mutant, 500 pM; ctDNA (2), two-base mutant, 500 pM; ctDNA (3), three-base mutant, 500 pM; no analyte. (d) The calibration column corresponding to the absorbance changes observed after a fixed time interval of 180 s. The error bars represent the standard deviation of the three measurements.

ctDNA (pM)				
Sample	Added	Found Mean <sup>a</sup> ± SD <sup>b</sup>	Recovery (%)	RSD <sup>c</sup> (%)
1	0	—	—	—
2	10	9.3 ± 0.5	98	5.38
3	50	44.5 ± 2.5	94	5.62
4	100	95.6 ± 5.4	101	5.65

**Table 1.** The proposed method for the detection of ctDNA in human blood plasma samples. <sup>a</sup>The mean of three determinations. <sup>b</sup>SD represents standard deviation. <sup>c</sup>RSD represents relative standard deviation.

suggested that this colorimetric sensing had good anti-interference performance in the detection of ctDNA in blood plasma samples. Hence, the approach had a great potential in the field of cancer early diagnosis and drug resistance in advanced cancers.

In conclusion, an ultrasensitive colorimetric sensing platform for circulating tumor DNA (ctDNA) was established, by using triple-helix DNA forming as a pivot to combine the hybridization chain reaction (HCR) amplification and the high peroxidase-like catalytic activity of the G-Quadruplex DNAzymes. This work provides a feasible method for the quantitative detection of ctDNA with high sensitivity, selectivity, and a detection limit of 0.1 pM ( $3\sigma/\text{slope}$ ), as well as satisfactory accuracy and reproducibility in human blood plasma samples. This design strategy can be used not only for ctDNA detection, but also can be further expanded to other biomarkers, involving other nucleic acid sequences, small molecules, proteins and cells, based on the elaborate design of the structures of capture probes. Although this study offers a costless and simple sensing platform for colorimetric and visual detection of ctDNA with a highly sensitive signal and negligible background, it still does not meet the needs of the clinical analysis. Therefore, the later studies will focus on the sensitivity and point-of-care testing of the strategies for nucleic acid detection.

## Methods

**Materials.** All oligonucleotides, 2,2'-azino-bis(3-ethylbenzothiozoline-6-sulfonic acid) (ABTS) and hemin (from bovine) were obtained from Sangon Biotech. Co. Ltd. (Shanghai, China). All reagents were of analytical grade and used as received without further purification. The stock solutions of all DNA molecules (100  $\mu$ M) were prepared in 20 mM Tris-Ac buffer (pH 7.4) and accurately quantified using UV-vis absorption spectrum with the following extinction coefficients (260 nm,  $M^{-1}cm^{-1}$ ): (A) 15400, (G) 11500, (C) 7400, (T) 8700. The stock solution of 4.0 mM hemin was prepared in dimethyl sulfoxide (DMSO), stored in darkness at  $-20^{\circ}C$ . All oligonucleotides solutions were diluted to required concentrations with the 20 mM Tris-Ac buffer (pH 7.4) and heated at  $90^{\circ}C$  for 10 min and then cooled down naturally to room temperature prior to use. Nanopure water (18.1 M $\Omega$ ) was used in this study produced by a 350 Nanopure water system (Guangzhou Crystalline Resource Desalination of Sea Water and Treatment Co. Ltd.). The sequences of all DNA molecules involved in this study were depicted as follows:

H<sub>1</sub>: 5'-ttc ctc TTC CTC TCT TCT CTC TCT tcc tct AGA GAG AGA AGA GAG GAA-3'  
 H<sub>2</sub>: 5'-AGA GAG AGA AGA GAG GAA gag gaa TTC CTC TCT TCT CTC TCT aga gga-3'  
 Initiator: 5'-AGA GAG AGA AGA GAG GAA GAG GAA-3'  
 L<sub>1</sub>: 5'-TGG GT TCT CTC CTT CTC CTT-3'  
 L<sub>2</sub>: 5'-TCT CCT TCT CTC TCT TGG GTA GGG CGG G-3'  
 dsDNA: 5'-TTC CTC TTC CTC TCT TCT CTC TCT TCC TCT-3'  
 3'-AAG GAG AAG GAG AGA AGA GAG AGA AGG AGA-5'  
 ctDNA: 5'-AGT GAT TTT AGA GAG AG-3'  
 ctDNA (1): 5'-AGT GAT TTA AGA GAG AG-3'  
 ctDNA (2): 5'-AGA GAT TTA AGA GAG AG-3'  
 ctDNA (3): 5'-AGA GAT TTA AGA GTG AG-3'  
 Capture: 5'-AGA GAG AGA AGA GAG GAA GAG GAA CTCTT CT CTC TCT AAA ATC ACT-3'

**Circular dichroism studies.** Circular dichroism (CD) spectroscopy experiments were measured on the Jasco J-810-150S spectropolarimeter at room temperature employing a quartz cell with a 0.1 cm path length. CD spectra were collected from 205 to 300 nm and with a scanning speed of 100 nm/min and 0.2 nm intervals. All CD spectra were baseline-corrected for signal contributions due to the buffer and were the average of at least three runs. The process was as follows: Samples H<sub>1</sub> + H<sub>2</sub>, L<sub>1</sub>, L<sub>2</sub>, L<sub>1</sub> + L<sub>2</sub>, Initiator + H<sub>1</sub> + H<sub>2</sub>, Initiator + H<sub>1</sub> + H<sub>2</sub> + L<sub>1</sub> + L<sub>2</sub>, prepared respectively in the Tris-Ac buffer (pH 7.4) containing 20 mM Tris, 0.25 mM spermine, 0.15  $\mu$ M Ag<sup>+</sup>, 0.10 MK<sup>+</sup>, were first incubated at  $37^{\circ}C$  for 3 h, and then transferred to  $25^{\circ}C$  water bath environment and hatched for 1 h prior to the CD measurement. The final concentrations of Initiator, H<sub>1</sub>, H<sub>2</sub>, L<sub>1</sub>, L<sub>2</sub>, involved in the CD studies were 5  $\mu$ M, 5  $\mu$ M, 5  $\mu$ M, 10  $\mu$ M, 10  $\mu$ M, respectively.

**Agarose gel electrophoresis.** The 2% agarose gel contained  $1 \times 4S$  Red Plus Nucleic Acid Stain, freshly prepared at laboratory, was used to perform the agarose gel electrophoresis analysis. The loading sample was mixed with 10  $\mu$ L of DNA sample, 2  $\mu$ L 6 loading buffer. The electrophoresis was carried out at a constant voltage of 100 V for 90 min, then the gel was imaged with a digital camera under UV irradiation.

**Native polyacrylamide gel electrophoresis (PAGE).** Nondenaturing polyacrylamide gel (15%) was prepared in 50 mM, pH 6.0 Tris-Ac buffer. Before loading samples, 10  $\mu$ L oligonucleotides was mixed with 2  $\mu$ L of 6  $\times$  loading buffer. Gel electrophoresis was run at  $25^{\circ}C$  for 2 h under a voltage of 90 V/cm at pH 6.0. After staining with 4S Red Plus Nucleic Acid Stain for 10 min and finally photographed with a digital camera under the illumination of UV light.

**Initiator assay procedure.** Samples contained different concentration Initiator, 0.2  $\mu$ M H<sub>1</sub>, 0.2  $\mu$ M H<sub>2</sub>, 0.4  $\mu$ M L<sub>1</sub>, 0.4  $\mu$ M L<sub>2</sub>, prepared in the Tris-Ac buffer (pH 7.4) containing 20 mM Tris, 0.25 mM spermine, 0.15  $\mu$ M Ag<sup>+</sup>, 0.10 MK<sup>+</sup>, 0.4  $\mu$ M hemin, were first incubated at  $37^{\circ}C$  for 3 h, and then transferred to  $25^{\circ}C$  water bath environment and hatched for 1 h. Finally, ABTS and H<sub>2</sub>O<sub>2</sub> were added, the final concentrations of each were 0.2 mM, 2.0 mM, respectively. The detection was carried out in the Kinetics mode of a UV-2550 UV-vis spectrophotometer (Shimadzu, Japan). The maximum absorption wavelength of the radical anion ABTS<sup>-</sup> (the oxidation product of ABTS<sup>2-</sup>) was about 420 nm.

**ctDNA assay procedure.** Samples contained different concentration ctDNA, 0.2  $\mu$ M Capture, 0.2  $\mu$ M H<sub>1</sub>, 0.2  $\mu$ M H<sub>2</sub>, 0.4  $\mu$ M L<sub>1</sub>, 0.4  $\mu$ M L<sub>2</sub>, prepared in the Tris-Ac buffer (pH 7.4) containing 20 mM Tris, 0.25 mM spermine, 0.15  $\mu$ M Ag<sup>+</sup>, 0.10 MK<sup>+</sup>, 0.4  $\mu$ M hemin, were first incubated at  $37^{\circ}C$  for 3 h, and then transferred to  $25^{\circ}C$  water bath environment and hatched for 1 h. Finally, ABTS and H<sub>2</sub>O<sub>2</sub> were added, the final concentrations of each were 0.2 mM, 2.0 mM, respectively. The detection was carried out in time course mode by monitoring the absorbance change at 420 nm on a UV-2550 UV-vis spectrophotometer (Shimadzu, Japan).

**Sample preparation.** The study protocol was approved by the ethic committee of Zhongshan Medical College, Sun Yat-sen University. Informed consent was obtained from each subject. All these experiments were performed in accordance with the relevant guidelines and regulations. Blood samples were gathered from healthy volunteers in our lab. Plasma samples were obtained by centrifugation of blood for about 5 min with a rotation rate of 3000–4000 rpm.

**Samples analysis.** DNA was isolated using the EZ-10 Spin Column Blood Genomic DNA Purification Kit (Sangon Biotech.) following the manufacturer's protocol. The procedure is depicted simply as follows: First,



100  $\mu$ L of PBS solution was added in 100  $\mu$ L plasma sample, and the solution was mixed. And then the above solution mixed with 20  $\mu$ L Proteinase K, 200  $\mu$ L Buffer CL was added, the obtained solution was stirred vigorously for well mixing, incubating for 10 min at 56 °C water bath. Second, 200  $\mu$ L ethyl alcohol was added to the above solution, and stirred vigorously for complete mixing. Transfer the prepared mixture to the spin column. Centrifuge for 1 min at 8,000 rpm. Discard the collection tube containing the flow-through solution. Place the column into a new 2 mL collection tube. Add 500  $\mu$ L of CW1 solution (with ethanol added). Centrifuge for 1 min at 10,000 rpm. Discard the flow-through and place the column back into the collection tube. Add 500  $\mu$ L of CW2 solution (with ethanol added) to the column. Centrifuge for 2 min at maximum speed ( $\geq$  12,000 rpm). Discard the collection tube containing the flow-through solution and transfer the column to a sterile 1.5 mL microcentrifuge tube (not included). Add 50  $\mu$ L of CE Buffer to the center of the column membrane to elute DNA. Incubate for 3 min at room temperature and centrifuge for 2 min at 12,000 rpm. Discard the purification column. Use the purified DNA immediately in downstream applications. The following DNA analysis is similar to the ctDNA assay procedure.

## References

- Bidard, F., Weigelt, B. & Reis-Filho, J. Going with the Flow: From Circulating Tumor Cells to DNA. *Sci. Transl. Med.* **5**, 207ps14 (2013).
- Newman, A. *et al.* An ultrasensitive method for quantitating circulating tumor DNA with broad patient coverage. *Nat. Med.* **20**, 548–554 (2014).
- Das, J., Ivanov, I., Sargent, E. H. & Kelley, S. DNA Clutch Probes for Circulating Tumor DNA Analysis. *J. Am. Chem. Soc.* **138**, 11009–11016 (2016).
- Jr, L. & Bardelli, A. Liquid Biopsies: Genotyping Circulating Tumor DNA. *J. Clin. Oncol.* **32**, 579–586 (2014).
- Monsur, A. *et al.* Rolling circle amplification: a versatile tool for chemical biology, materials science and medicine. *Chem. Soc. Rev.* **43**, 3324–3341 (2014).
- Zhang, J. *et al.* Hairpin DNA-templated silver nanoclusters as novel beacons in strand displacement amplification for microRNA detection. *Anal. Chem.* **88**, 1294–1302 (2016).
- Garcia, E., Farnleitner, A., Mach, R., Krska, R. & Brunner, K. A rapid genomic DNA extraction method and its combination with helicase dependent amplification for the detection of genetically modified maize. *Anal. Methods*, **8**, 136–141 (2016).
- Dirks, R. & Pierce, N. Triggered amplification by hybridization chain reaction. *Proc. Natl. Acad. Sci. USA* **101**, 15275–15278 (2004).
- Choi, H., Beck, V. & Pierce, N. Next-Generation *in Situ* Hybridization Chain Reaction: Higher Gain, Lower Cost, Greater Durability. *ACS Nano* **8**, 4284–4294 (2014).
- Ikbal, J., Lim, G. & Gao, Z. The hybridization chain reaction in the development of ultrasensitive nucleic acid assays. *Trends Anal. Chem.* **64**, 86–99 (2015).
- Li, X., Wang, Y., Wang, L. & Wei, Q. A surface plasmon resonance assay coupled with a hybridization chain reaction for amplified detection of DNA and small molecules. *Chem. Commun.* **50**, 5049–5052 (2014).
- Ding, X. *et al.* An enzyme-free surface plasmon resonance biosensing strategy for detection of DNA and small molecule based on nonlinear hybridization chain reaction. *Biosens. Bioelectron.* **87**, 345–351 (2017).
- Liu, P. *et al.* Enzyme-Free Colorimetric Detection of DNA by Using Gold Nanoparticles and Hybridization Chain Reaction Amplification. *Anal. Chem.* **85**, 7689–7695 (2013).
- Miao, P., Tang, Y. & Yin, J. MicroRNA detection based on analyte triggered nanoparticle localization on a tetrahedral DNA modified electrode followed by hybridization chain reaction dual amplification. *Chem. Commun.* **51**, 15629–15632 (2015).
- Miao, J. *et al.* A plasmonic colorimetric strategy for visual miRNA detection based on hybridization chain reaction. *Sci Rep.* **6**, 32219 (2016).
- Xie, P. *et al.* Highly sensitive detection of lipopolysaccharides using an aptasensor based on hybridization chain reaction. *Sci Rep.* **6**, 29524 (2016).
- Zou *et al.* Colorimetric sensing platform based upon recognizing hybridization chain reaction product with oligonucleotide modified gold nanoparticles through triplex formation *Nanoscale* **9**, 1986–1992 (2017).
- Deng, M., Zhang, D., Zhou, Y. & Zhou, X. Highly Effective Colorimetric and Visual Detection of Nucleic Acids Using an Asymmetrically Split Peroxidase DNzyme. *J. Am. Chem. Soc.* **130**, 13095–13102 (2008).
- Ihara, T., Ishii, T., Araki, N., Wilson, A. & Jyo, A. Silver Ion Unusually Stabilizes the Structure of a Parallel-Motif DNA Triplex. *J. Am. Chem. Soc.* **131**, 3826–3827 (2009).
- Ge, Z. *et al.* Hybridization Chain Reaction Amplification of MicroRNA Detection with a Tetrahedral DNA Nanostructure-Based Electrochemical Biosensor. *Anal. Chem.* **86**, 2124–2130 (2014).
- Niu, S., Jiang, Y. & Zhang, S. Fluorescence detection for DNA using hybridization chain reaction with enzyme-amplification. *Chem. Commun.* **46**, 3089–3091 (2010).
- Chen, Y. *et al.* *In Situ* Hybridization Chain Reaction Amplification for Universal and Highly Sensitive Electrochemiluminescent Detection of DNA. *Anal. Chem.* **84**, 7750–7755 (2012).
- Li, R. *et al.* G-quadruplex DNzymes-induced highly selective and sensitive colorimetric sensing of free heme in rat brain. *Analyst* **139**, 1993–1999 (2014).
- Li, R., Xiong, C., Xiao, Z. & Ling, L. Colorimetric detection of cholesterol with G-quadruplex-based DNzymes and ABTS<sup>2-</sup>. *Anal. Chim. Acta* **724**, 80–85 (2012).
- Manzini, G., Xodo, L. & Gasparotto, D. Triple Helix Formation by Oligopurine-oligopyrimidine DNA Fragments. *J. Mol. Biol.* **213**, 833–843 (1990).
- Feng, L., Huang, Z., Ren, J. & Qu, X. Toward site-specific, homogeneous and highly stable fluorescent silver nanoclusters fabrication on triplex DNA scaffolds. *Nucl. Acids Res* **40**, e122 (2012).
- Nakayama, S. & Sintim, H. Colorimetric Split G-Quadruplex Probes for Nucleic Acid Sensing: Improving Reconstituted DNzyme's Catalytic Efficiency via Probe Remodeling. *J. Am. Chem. Soc.* **131**, 10320–10333 (2009).
- Dong, J., Cui, X., Deng, Y. & Tang, Z. Amplified detection of nucleic acid by G-quadruplex based hybridization chain reaction. *Biosens. Bioelectron.* **38**, 258–263 (2012).
- He, H. *et al.* Unusual sequence length-dependent gold nanoparticles aggregation of the ssDNA sticky end and its application for enzyme-free and signal amplified colorimetric DNA detection. *Sci. Rep.* **6**, 30878 (2016).
- Stoltenburg, R., Krafčiková, P., Víglašký, V. & Strehlitz, B. G-quadruplex aptamer targeting Protein A and its capability to detect *Staphylococcus aureus* demonstrated by ELONA. *Sci. Rep.* **6**, 33812 (2016).
- Yang, Z., Castrignanò, E., Estrela, P., Frost, C. G. & Kasprzyk-Hordern, B. Community Sewage Sensors towards Evaluation of Drug Use Trends: Detection of Cocaine in Wastewater with DNA-Directed Immobilization Aptamer Sensors. *Sci. Rep.* **6**, 21024 (2016).
- Chang, Y. *et al.* Rapid single cell detection of *Staphylococcus aureus* by aptamer-conjugated gold nanoparticles. *Sci. Rep.* **3**, 1863 (2013).

33. Zhou, Q. *et al.* Detection of Circulating Tumor DNA in Human Blood via DNA Mediated Surface-Enhanced Raman Spectroscopy of Single-Walled Carbon Nanotubes. *Anal. Chem.* **88**, 4759–4765 (2016).
34. Nguyen, A. H. & Sim, S. J. Nanoplasmonic biosensor: Detection and amplification of dual bio-signatures of circulating tumor DNA. *Biosens. Bioelectron.* **67**, 443–449 (2015).
35. Das, J. *et al.* An electrochemical clamp assay for direct, rapid analysis of circulating nucleic acids in serum. *Nat. Chem.* **7**, 569–575 (2015).

### Acknowledgements

This work was supported by the National Natural Science Foundation of China (Grant No. 21375153) and the Natural Science Foundation of Guangdong Province (Grant No. 2016A030310188).

### Author Contributions

R.L. and L.Z. carried out the experiments, performed the data analysis. R.L. wrote the manuscript. L.Z., Y.L. and M.Z. performed the data analysis. L.L. designed the experiments and analyzed the results.

### Additional Information

**Supplementary information** accompanies this paper at <http://www.nature.com/srep>

**Competing Interests:** The authors declare no competing financial interests.

**How to cite this article:** Li, R. *et al.* Ultrasensitive colorimetric detection of circulating tumor DNA using hybridization chain reaction and the pivot of triplex DNA. *Sci. Rep.* **7**, 44212; doi: 10.1038/srep44212 (2017).

**Publisher's note:** Springer Nature remains neutral with regard to jurisdictional claims in published maps and institutional affiliations.



This work is licensed under a Creative Commons Attribution 4.0 International License. The images or other third party material in this article are included in the article's Creative Commons license, unless indicated otherwise in the credit line; if the material is not included under the Creative Commons license, users will need to obtain permission from the license holder to reproduce the material. To view a copy of this license, visit <http://creativecommons.org/licenses/by/4.0/>

© The Author(s) 2017